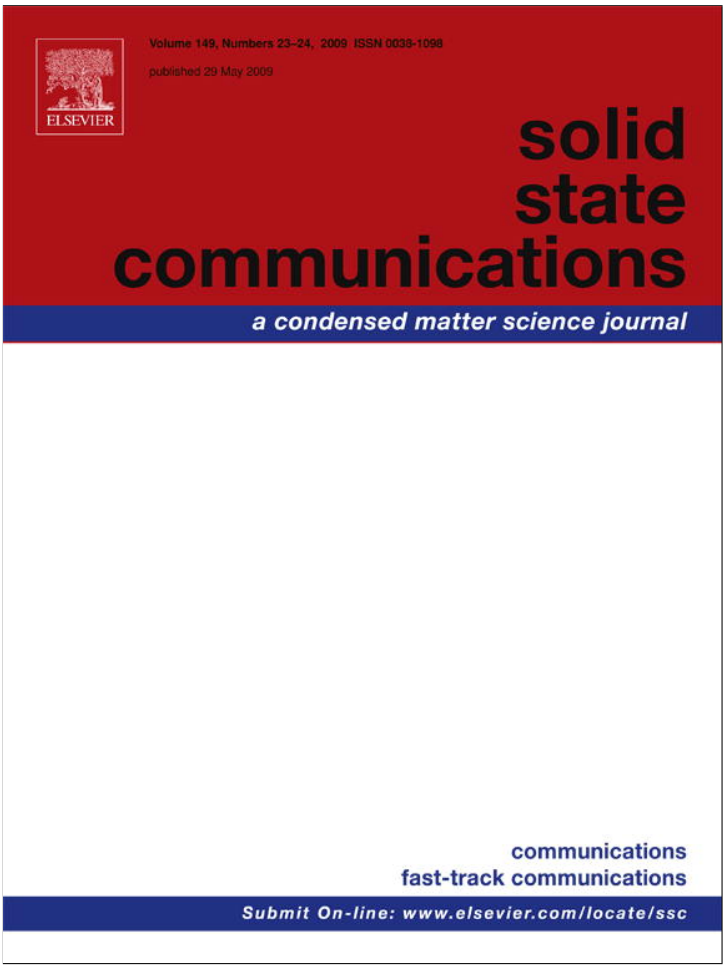

Solid State Communications 149 (2009) 915–918

Contents lists available at ScienceDirect

Solid State Communications

journal homepage: www.elsevier.com/locate/ssc

Dynamic process of photovoltaic effect in $La_{0.9}Sr_{0.1}MnO_3/SrNb_{0.01}Ti_{0.99}O_3$ heterojunction

Leng Liao, Kui-juan Jin *, Hui-bin Lu, Peng Han, Meng He, Guo-zhen Yang

Beijing National Laboratory for Condensed Matter Physics, Institute of Physics, Chinese Academy of Sciences, Beijing 100190, China

ARTICLE INFO

Article history:
Received 26 June 2008
Received in revised form
23 March 2009
Accepted 24 March 2009 by A. Morpurgo
Available online 29 March 2009

PACS:
73.40.Lq
72.40.+w
78.20.Bh

Keywords:
A. Heterojunction
D. Photoconductivity and photovoltaics

ABSTRACT

The dynamic process of photoelectric effects in the $La_{0.9}Sr_{0.1}MnO_3/SrNb_{0.01}Ti_{0.99}O_3$ heterostructure is theoretically revealed by solving equations consisting of *time dependent* drift–diffusion, Richardson thermionic emission current, and Shockley–Read–Hall recombination. The calculated *time dependent* evolution of photovoltage and the variation of carrier concentration are obtained. Present results indicate that a smaller parallel resistance should result in faster photoelectric response, but reduce the peak value of the photovoltage in a $La_{0.9}Sr_{0.1}MnO_3/SrNb_{0.01}Ti_{0.99}O_3$ heterojunction. In addition, the increase of the carrier mobilities induced by applying higher energy photons can decrease the rise time but increase the peak value of the photovoltage.

Many novel photo-induced properties, such as the photo-induced insulator-to-metal transition [1], the photo-induced spin-state transition [2], and persistent photoconductivity [3], have been found in perovskite oxide materials. Light can manipulate the concentration and the spin states of carriers in perovskite oxides [4,2], thus it is possible to create optical–magnetic devices with high density and high speed. Recently, much effort has been devoted to the photoelectric effect of perovskite oxide heterojunctions. A photovoltaic pulse of ~8 ms full width at half-maximum (FWHM) has been observed in a $La_{0.29}Pr_{0.38}Ca_{0.33}MnO_3/SrNb_{0.005}Ti_{0.995}O_3$ heterojunction [5]. An ultrafast photovoltaic pulse of ~650 ps FWHM in $La_{0.7}Sr_{0.3}MnO_3/Si$ heterojunction has been reported [6], which suggests a potential application of the high speed photoelectric devices made by perovskite oxide heterojunctions. In our previous work [7], we observed unusual lateral photoelectric effect in the $La_{0.9}Sr_{0.1}MnO_3/SrNb_{0.01}Ti_{0.99}O_3$ and $La_{0.7}Sr_{0.3}MnO_3/Si$ heterojunctions, and proposed it as a Dember effect. However, those works are mainly experimental. So far, due to the complexity of perovskite oxides, no relative theoretical work on the photoelectric effect in perovskite oxide heterojunctions has been reported yet.

In this letter, based on the *time dependent* drift–diffusion model [8], electron and hole continuity equation, Poisson equation, Richardson thermionic emission current [9], and Shockley–Read–Hall recombination process [10], the dynamic photoelectric process in a $La_{0.9}Sr_{0.1}MnO_3/SrNb_{0.01}Ti_{0.99}O_3$ (LSMO/SNTO) heterojunction is revealed from a theoretical aspect. The calculated results confirm that a smaller connected parallel resistance can increase the speed of the photoelectric response of a LSMO/SNTO heterojunction. Therefore, parallel resistance is one of the key factors affecting the response speed and sensitivity of the photoelectric effect in a LSMO/SNTO heterojunction. Moreover, the present results reveal that the photovoltaic signal and response speed increase with an increase of the carrier mobility induced by higher energy photons. Thus high energy photon excitation can increase the speed and sensitivity of the photoelectric response in a LSMO/SNTO heterojunction.

The system studied in this work is a heterojunction with a uniform and vertical irradiation on the surface of the p-type region as shown in Fig. 1. Carrier movement is assumed just along the c-direction of the heterojunction. Therefore, the dynamic photoelectric process in this system is treated as a one-dimensional process. Here, we introduce a one-dimensional *time dependent* drift–diffusion model to give a description of the dynamic photoelectric process in perovskite heterojunctions.

In this model, the Poisson equation and *time dependent* continuity equations are presented as follows,

$$\frac{\partial^2\phi(x,t)}{\partial x^2} = -\frac{e}{\varepsilon(x)}[p(x,t) - n(x,t) + N], \quad (1)$$

* Corresponding author. Tel.: +86 10 82648099.
E-mail address: kjjin@aphy.iphy.ac.cn (K.-j. Jin).

0038-1098/$ – see front matter
doi:10.1016/j.ssc.2009.03.029

Table 1
The material parameters.

	$La_{0.9}Sr_{0.1}MnO_3$	$SrNb_{0.01}Ti_{0.99}O_3$
Dielectric constant (ε_0)	10	150
Electron mobility ($cm^2/(V.s)$)	10	33[a]
Hole mobility ($cm^2/(V.s)$)	1.8[a]	6
Band gap (eV)	1.0	2.8

[a] Parameters taken from Ref. [14].

$$\frac{\partial n(x,t)}{\partial t} = -\mu_n n(x,t)\frac{\partial^2\phi(x,t)}{\partial x^2} - \mu_n\frac{\partial n(x,t)}{\partial x}\frac{\partial\phi(x,t)}{\partial x} + \frac{kT\mu_n}{e}\frac{\partial^2 n(x,t)}{\partial x^2} + G(x,t) - R(x,t), \quad (2)$$

$$\frac{\partial p(x,t)}{\partial t} = \mu_p p(x,t)\frac{\partial^2\phi(x,t)}{\partial x^2} + \mu_p\frac{\partial p(x,t)}{\partial x}\frac{\partial\phi(x,t)}{\partial x} + \frac{kT\mu_p}{e}\frac{\partial^2 p(x,t)}{\partial x^2} + G(x,t) - R(x,t), \quad (3)$$

where $\phi(x,t)$, $p(x,t)$ and $n(x,t)$ represent the electrostatic potential, hole and electron concentrations, e, ε and N denote electron charge, dielectric permittivity, and net ionized impurity concentrations, respectively; and μ_p and μ_n denote hole and electron mobilities, respectively. The interface condition for solving the Poisson equation Eq. (1) is taken as $\phi(x_{inter}-\delta,t) = \phi(x_{inter}+\delta,t)$, where x_{inter} denotes the position of the interface and δ is infinitesimal. Furthermore, because the drift–diffusion model cannot be used to describe the carrier movement across the interface of the heterojunction, the Richardson thermionic emission current [9] is used to treat the transport process at the interface of the heterojunction. And the Richardson thermionic emission current [9] is employed as an interface condition for solving *time dependent* continuity equations (Eqs. (2), (3)). k and T denote the Boltzmann constant and temperature, respectively. In the calculation, T is taken as 300 K, $G(x,t)$ is the photo-excited electron–hole pair generation rate, which was taken as $G(x,t) = I_0(t)\alpha\beta\exp(-\alpha x)$, where $I_0(t)$ denotes the intensity of incident photon flux, taken as $2.6\times10^{23}/cm^2\cdot s$, by considering the incident energy (0.1 mJ) of the laser pulse, wave length (308 nm), the irradiated area of the heterojunction (0.3 cm^2), and the laser pulse duration (25 ns) in the calculation, α denotes the photon absorption coefficient, and β denotes the quantum efficiency, respectively. α was taken as 1.5×10^5 cm^{-1} and 1.2×10^5 cm^{-1} for LSMO [11] and SNTO [12], respectively. β was set as 0.05 and 0.088 for LSMO and SNTO, respectively, in our calculation. $R(x,t)$ denotes recombination rate presented by Shockley–Read–Hall (SRH) model [10]. In the calculation, $N = -1.0\times10^{19}/cm^3$ in LSMO and $N = 1.0\times10^{20}/cm^3$ in SNTO, taken according to our Hall measurement, some other important parameters are shown in Table 1, and the others are all taken from Ref. [13]. The initial values ($t=0$): $\phi(x,0)$, $p(x,0)$ and $n(x,0)$ for solving Eqs. (1)–(3) were obtained by solving the Poisson equation coupled with the Boltzmann approximation [8].

The LSMO/SNTO heterojunction was fabricated by depositing a 40 nm thick p-type LSMO layer on n-type SNTO (0 0 l) substrate by laser molecular-beam epitaxy (Laser-MBE). An *in situ* reflection high-energy electron diffraction (RHEED) system was used to monitor the growth process of the LSMO film. A resistance of 50 Ω is connected to this LSMO/SNTO heterojunction as shown in Fig. 1, through setting indium electrodes on the LSMO surface and the opposite surface of SNTO. A XeCl pulsed laser (wavelength of 308 nm, repetition rate of 1 Hz and duration of 20 ns) is irradiated on the surface of the LSMO layer. At the same time, the induced *PV* was measured by a 500 MHz oscilloscope.

The experimental and calculated time dependent *PV* curves are shown in Fig. 1(a) and (b), respectively. Due to the complication of light-absorption and carrier-recombination in perovskite oxide

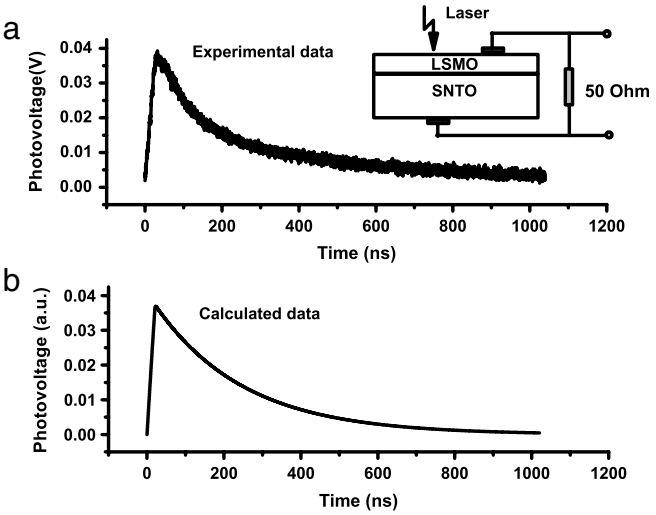

Fig. 1. (a) The experimental *PV*-time curves in a LSMO/SNTO heterojunction. (b) The calculated *PV*-time curves in a LSMO/SNTO heterojunction. Laser is on at 0 ns and off at 20 ns. The peak of the curve locates at ∼40 ns.

heterojucntion, accurate relative parameters are difficult to obtain, especially the quantum efficiency β. According to our calculation, these parameters only affect the photovoltaic intensity. While we are only concerned with the evolution process of the photovoltage, we give a comparison between the calculated and experimental data of the photovoltage with an arbitrary unit (a. u.). In Fig. 1, both calculated and experimental photovoltages rise to a peak at ∼40 ns and decay exponentially. After ∼1000 ns, both of them decrease to 0. Therefore, regardless of the intensity of the photovoltage, the calculated evolution of the photovoltage shows good agreement with the experimental data. This result confirms the validity of the present model applied to the perovskite oxide heterojunction.

The process of the photoelectric effect in a LSMO/SNTO heterojunction is considered as the charging and discharging of a resistance–capacitance (RC) circuit. In Fig. 2, the calculated evolution of the variation of carrier concentration relative to that of the initial state exhibits such a *time dependent* charging and discharging process in the LSMO/SNTO heterojunction. Fig. 2(a) and (b) show the evolution of the variation of electron and hole concentration in the period of 5–20 ns, respectively, while the laser is on. By the built-in field in the space-charge region of the heterojunction, the photo-excited electrons and holes accumulate in the $n(x > 40$ nm) and $p(x < 40$ nm) region respectively. It approximates a process of charging capacitance. Fig. 2(c) and (d) show the evolution of the variation of electron and hole concentration in the period of 100–700 ns, respectively, while the laser is off. Due to photo-excited carriers leaking out through the parallel resistance, the electrons and holes accumulating in the n and p regions are gradually reduced. It approximates a process of discharging.

In a RC circuit, the decay of voltage is expressed as an exponential decay:

$$V(t) = V_0\exp(-t/RC), \quad (4)$$

where t, R and C denote time, resistance and capacitance, respectively, V and V_0 are the potential difference and the initial potential difference between two capacitance's electrodes, respectively. According to Eq. (4), the speed of decay of the potential difference increases with the decrease of R. Correspondingly, for the photoelectric effect of the LSMO/SNTO heterojunction, the decrease of parallel resistance can increase the speed of photoelectric response of the heterojunction, which has been proved in a similar experiment for photoelectric response in the heterojunction of

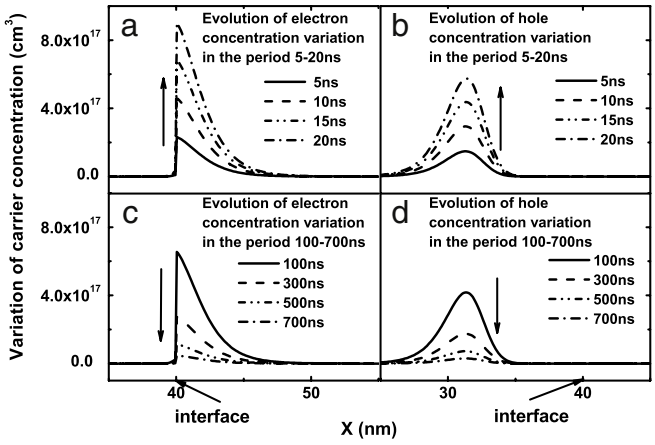

Fig. 2. The evolution of carrier concentration variation in the photoelectric process. (a) and (b) show the evolution of electron and hole concentration variation in the period of 5–20 ns while the laser is on, respectively. (c) and (d) show the evolution of electron and hole concentration variation in the period of 100–700 ns while the laser is off and the PV is decaying, respectively.

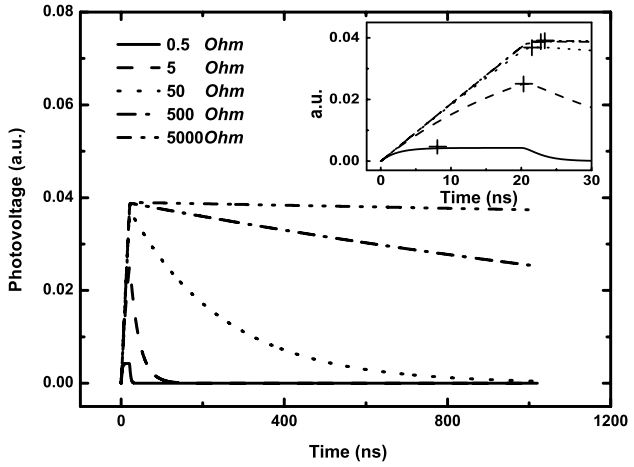

Fig. 3. The calculated *PV*-time curves of the LSMO/SNTO heterojunction with various parallel resistances: 0.5, 5, 50, 500 and 5000 Ω. The inset shows the time dependent rising of the *PV* in the time scale of 0-30 ns, and the *PV* peaks are marked by crosses.

$La_{0.7}Sr_{0.3}MnO_3$/Si [7]. Fig. 3 shows the calculated *time dependent PV* evolution with various parallel resistances. The smaller the resistance, the faster the decay of *PV*. However, the peak value of *PV* decreases with the decrease of parallel resistance, because more photo-excited carriers can leak out through the smaller resistance during the irradiation. In addition, with the decreasing of the parallel resistance, the rise time of *PV* decreases as shown in the inset of Fig. 3. This is because the LSMO/SNTO heterojunction with a smaller parallel resistance can reach photoelectric saturation earlier, and this saturation occurs when the carriers leaking out are in equilibrium with the carriers induced by photons. Therefore, the speed of photoelectric response increases and the photoelectric sensitivity decreases with decreasing parallel resistance, respectively.

If the energy of photons irradiating onto the perovskite oxide heterojunction is high enough, the excess energy of the excited carriers will transform into their kinetic energy. Consequently, the average mobilities of both electron and hole are increased. For studying the effect of photon energy on the photoelectric response of a LSMO/SNTO heterojunction, we also calculated the *PV* evolvement for a laser pulse irradiation with 0.02 ns duration but various photon energies on a LSMO/SNTO heterostructure with 500 nm thick LSMO layer connected with a 0.2 Ω parallel

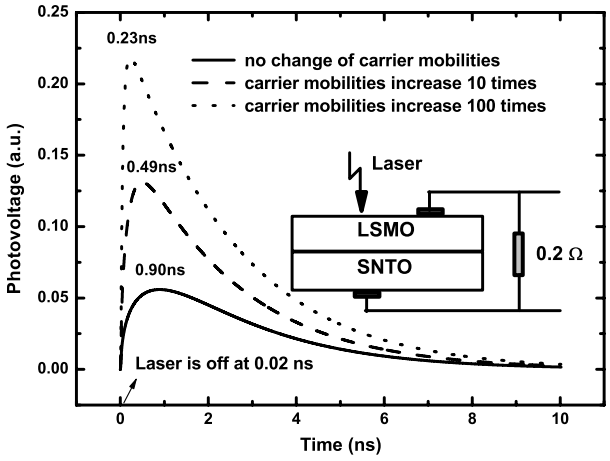

Fig. 4. The calculated *PV*-time curves of a LSMO/SNTO heterojunction with various carrier mobilities. The laser is on at 0 ns and off at 0.02 ns. The positions of peaks are marked out at the respective peak.

resistance. The calculated results with various carrier mobilities which correspond to various photon energies are exhibited in Fig. 4. As a higher photon energy corresponds to higher carrier mobilities, the increase of photon energy is indirectly manifested by an increase in carrier mobility. The increase of carrier mobility decreases the diffusing time of photo-excited carriers from the surface to the space-charge region. For the RC circuit, it means that the time for charging the capacitance is reduced. Therefore, in Fig. 4, the carrier mobilities increase 10 times and 100 times and then the rise time of *PV* is reduced to 0.49 ns and 0.23 ns from 0.9 ns, respectively. In other words, a higher photon energy induces a shorter rise time. Moreover, an increase in carrier mobility decreases the charging time of the heterojunction, and the carriers leaking out in the period of charging decrease. Accordingly, the *PV* peak increases with increasing mobility as shown in Fig. 4. It means that the increase of photon energy can increase the sensitivity of the LSMO/SNTO heterojunction. In addition, we found that there is no strong relation between the decay time of *PV* and the carrier mobility of the heterojunction because the increase of carrier mobility cannot change the capacitance of the heterojunction. Therefore, it is predicted that applying high energy photons on to the heterojunction to excite electrons can increase both sensitivity and the speed of photoelectric response. Or, in other words, using a heterostructure which consists of materials with high mobility also improves both the sensitivity and the speed of photoelectric response.

In summary, on the basis of a time dependent drift–diffusion model and the hot current model, the dynamic photoelectric process of a LSMO/SNTO heterojunction is revealed. The calculated results agree well with experimental data. The calculated results indicate that a decrease in parallel resistance can increase the speed of photoelectric response but reduce the photoelectric sensitivity. In addition, the increase of carrier mobility induced by higher energy photons can increase both the sensitivity and speed of photoelectric response in a LSMO/SNTO heterojunction.

Acknowledgement

This work has been supported by the National Natural Science Foundation of China and National Basic Research Program of China.

References

[1] K. Miyano, T. Tanaka, Y. Tomioka, Y. Tokura, Phys. Rev. Lett. 78 (1997) 4527.
[2] R.L. Zhang, J.M. Dai, W.H. Song, Y.Q. Ma, J. Yang, Y.P. Sun, J. Phys.: Condens. Matter 16 (2004) 2245.

[3] J.M. Dai, W.H. Song, J.J. Du, J.N. Wang, Y.P. Sun, Phys. Rev. B 67 (2003) 144405.
[4] H. Katu, H. Tanaka, T. Kawai, Appl. Phys. Lett. 76 (2000) 3245.
[5] J.R. Sun, C.M. Xiong, B.G. Shen, P.Y. Wang, Y.X. Weng, Appl. Phys. Lett. 84 (2004) 2611.
[6] H.B. Lu, K.J. Jin, Y.H. Huang, M. He, K. Zhao, B.L. Cheng, Z.H. Chen, Y.L. Zhou, S.Y. Dai, G.Z. Yang, Appl. Phys. Lett. 86 (2005) 241915.
[7] K.J. Jin, K. Zhao, H.B. Lu, L. Liao, G.Z. Yang, Appl. Phys. Lett. 97 (2007) 081906.
[8] S. Selberherr, Analysis and Simulation of Semiconductor Devices, Springer-Verlag, Wien, New York, 1984, 128.
[9] K Yang, J.R. East, G.I. Haddad, Solid-State Electron. 36 (1993) 321.
[10] W. Shockley, W.T. Read, Phys. Rev. 87 (1952) 835.
[11] M.W. Kim, P. Murugavel, S. Parashar, J.S. Lee, T.W. Noh, New J. Phys. 6 (2004) 156.
[12] M.I. Cohen, R.F. Blunt, Phys. Rev. 168 (1968) 929.
[13] P. Han, K.J. Jin, H.B. Lu, Q.L. Zhou, Y.L. Zhou, G.Z. Yang, Appl. Phys. Lett. 91 (2007) 182102.
[14] K. Zhao, Y.H. Huang, Q.L. Zhou, K.J. Jin, H.B. Lu, M. He, B.L. Cheng, Y.L. Zhou, Z.H. Chen, G.Z. Yang, Appl. Phys. Lett. 86 (2005) 221917.